2019

In vitro metabolism of the synthetic cannabinoids PX-1, PX-2, PX-3 and a comparison of their clearance rates in human liver microsomes

Travon Cooman
West Virginia University (WVU), tc0057@mix.wvu.edu

2019

In vitro metabolism of the synthetic cannabinoids PX-1, PX-2, PX-3 and a comparison of their clearance rates in human liver microsomes

Travon Cooman

In vitro metabolism of the synthetic cannabinoids PX-1, PX-2, PX-3 and a comparison of their clearance rates in human liver microsomes

Travon Cooman

Thesis submitted

to the Eberly College of Arts and Sciences

at West Virginia University

in partial fulfillment of the requirements for the degree of

Master of Science in

Forensic and Investigative Science

Suzanne Bell, Ph.D., Chair
Luis Arroyo, Ph.D.
Jonathan Boyd, Ph.D.

Department of Forensic and Investigative Science

Morgantown, West Virginia

2019

Keywords: synthetic cannabinoids, clearance rate, high resolution mass spectrometry, binding affinity, marker metabolites

Abstract

In vitro metabolism of the synthetic cannabinoids PX-1, PX-2, PX-3 and a comparison of their clearance rates in human liver microsomes

Travon Cooman

Detection of SCs in body fluids continue to be a challenge because of limited metabolism data, lack of standards and reference mass spectrometry data. *In vivo* and *in vitro* experiments help elucidate metabolite markers for novel psychoactive substances and can prompt synthesis of standards to verify proposed metabolites. In this study, metabolism of three SCs N-(1-amino-1-oxo-3-phenylpropan-2-yl)-1-(5-fluoropentyl)-1H-indole-3-carboxamine (**PX-1**), N-(1-amino-1-oxo-3-phenylpropan-2-yl)-1-(5-fluropentyl)-1H-indazole-3-carboxamide (**PX-2**), and N-(1-amino-1-oxo-3-phenylpropan-2-yl)-1-(cyclohexylmethyl)-1H-indazole-3-carboxamide (**PX-3**) were investigated using human liver microsomes. Previous studies showed PX-3 as the most potent CB_1 and CB_2 receptor agonist.

Half-life and clearance data were acquired using liquid chromatography- tandem mass spectrometry. Metabolite elucidation was performed using liquid chromatography high-resolution mass spectrometry in combination with Compound Discoverer®. A previously characterized SC, NM2201 was used as a control.

The calculated half-lives were 15.1±1.02, 3.4±0.27, 5.2±0.89 minutes for PX-1, PX-2, and PX-3 respectively. The calculated intrinsic clearance values were 0.046, 0.202, 0.133 mL/ min mg for PX-1, PX-2 and PX-3 respectively. Four metabolites of PX-1, six metabolites of PX-2 and five phase I metabolites of PX-3 were detected. Oxidative deamination was the common biotransformation between the three compounds. Elucidation of marker metabolites are useful to confirm consumption of SCs.

Acknowledgments

Throughout my life, many people have contributed to my success and this thesis would not be possible without their encouragement.

First and foremost, thanks to my advisor Dr. Suzanne Bell for first agreeing to accept me into her lab and her unwavering support throughout my time as a master's student. Her enthusiasm for science and relaxed personality will always remain with me. She fostered an environment that encouraged me to make my own mistakes and learn from them even though these mistakes happened sometimes when using expensive analytical instruments.

To my committee members Dr. Luis Arroyo and Dr. Jonathan Boyd, I appreciate your willingness to mentor me and help me think critically about my research.

Thanks to Dr. Glen Jackson who helped me determine structures of MS fragments.

A very special thanks to Matthew Maust and Yan Pan for helping me understand how to use the necessary instruments and software required to complete this thesis.

To Sandra Majuta at WVU Shared Research Facilities, thank you for assisting me with troubleshooting the Orbitrap.

My colleagues, Tyler Davidson and Bill Feeney, thank you for always listening to me and helping me think through challenging problems.

My Chicago family, Cindi and Ed Woods, I will forever be grateful to you for your support. My mom and dad, although I had to survive without a tasty home cooked meal, you always sent me sunshine from beautiful St. Lucia.

Table of Contents

Table of Figures

List of Abbreviations

5FPB22 met	1-(5-fluoropentyl)-1H-indole-3-carboxylic acid
APP-1	(1-(cyclohexylmethyl)-1H-indazole-3-carbonyl)phenylalanine
APP-2/3/4/5	((1-((hydroxycyclohexylmethyl)methyl)-1H-indazole-3-carbonyl)phenylalanine
CE	Collision energy
Cell Acc	Cell accelerator voltage
CYP	Cytochrome P450
dd	Data dependent
Frag	Fragmentor voltage
FU-1	(1-(5-fluoropentyl)-1H-indazole-3-carbonyl)phenylalanine
FU-2	(1-(5-hydroxypentyl)-1H-indazole-3-carbonyl)phenylalanine
FU-3	N-(1-amino-1-oxo-3-phenylpropan-2-yl)-1-(5-hydroxypentyl)-1H-indazole-3-carboxamide
HLM	Human liver microsomes
HPLC	High pressure liquid chromatography
LC/MS	Liquid chromatography mass spectrometry
LOD	Limit of Detection
MRM	Multiple reaction monitoring
MS	Mass spectrometry
NADPH	Nicotinamide adenine dinucleotide phosphate
NM2201	Naphthalen-1-yl 1-(5-fluoropentyl)-1H-indole-3-carboxylate
NPS	Novel psychoactive substance
PB22-d_9	1-pentyl-2,2',3,3',4,4',5,5-d_9-8-quinolinyl ester-1H-indole-3-carboxylic acid
PX-1 or 5-fluoro APP-PICA or SRF-30	N-(1-amino-1-oxo-3-phenylpropan-2-yl)-1-(5-fluoropentyl)-1H-indole-3-carboxamine
PX-2 or 5- fluoro APP-PINACA or FU-PX	N-(1-amino-1-oxo-3-phenylpropan-2-yl)-1-(5-fluropentyl)-1H-indazole-3-carboxamide
PX-3 or APP-CHMINACA	N-(1-amino-1-oxo-3-phenylpropan-2-yl)-1-(cyclohexylmethyl)-1H-indazole-3-carboxamide

SC	Synthetic Cannabinoid
SIM	Selected Ion Monitoring
SRF-1	N-(1-amino-1-oxo-3-phenylpropan-2-yl)-1-(5-hydroxypentyl)-1H-indole-3-carboxamide
SRF-2	N-(1-amino-1-oxo-3-phenylpropan-2-yl)-1H-indole-3-carboxamide
SRF-3	(1-(5-fluoropentyl)-1H-indole-3-carbonyl)phenylalanine
SRF-4	(1-(5-hydroxypentyl)-1H-indole-3-carbonyl)phenylalanine
SWGTOX	Scientific Working Group for Forensic Toxicology
AB-PINACA	N-(1-amino-3-methyl-1-oxobutan-2-yl)-1-pentyl-1H-indazole-3-carboxamide

Introduction

This thesis is a summary of a manuscript submitted to the Journal of Forensic Toxicology in February 2019.

New synthetic cannabinoids (SCs) are being constantly introduced into the clandestine market to evade detection by law enforcement and researchers. As a result, analytical labs often do not have access to reference mass spectra for newer cannabinoids, let alone access to reference standards for the parent or metabolites. The extensive metabolism of parent compounds make detection in body fluids challenging, but *in vitro* studies can elucidate marker metabolites.

The primary goal of this work was to calculate half-life, clearance and to identify metabolites to the extent possible of three previously uncharacterized SCs. Human liver microsomes, an affordable *in vitro* alternative for drug biotransformation and pharmacokinetics studies was utilized for this purpose. Microsomes are rich in cytochrome P450 (CYP) enzymes responsible for the metabolism of most drugs.

The three synthetic cannabinoids used in this study, N-(1-amino-1-oxo-3-phenylpropan-2-yl)-1-(5-fluoropentyl)-1H-indole-3-carboxamine (PX-1 or 5-fluoro APP-PICA or SRF-30), N-(1-amino-1-oxo-3-phenylpropan-2-yl)-1-(5-fluropentyl)-1H-indazole-3-carboxamide (PX-2 or 5-fluoro APP-PINACA or FU-PX), and N-(1-amino-1-oxo-3-phenylpropan-2-yl)-1-(cyclohexylmethyl)-1H-indazole-3-carboxamide (PX-3 or APP-CHMINACA) were first detected in 2015.

The structures of the 15 metabolites useful in toxicology analysis were tentatively identified using high resolution mass spectrometry (HRMS), whereas half-life and clearance were investigated using a triple quadrupole system.

Literature Review

Preface

Synthetic Cannabinoids are a class of novel psychoactive substances (NPS) which are used for their psychoactive effects [1]. Whenever a NPS is scheduled the structure is easily modified so that it goes undetected by Law Enforcement [2]. Toxicologists are faced with the challenge of identifying NPS as they have become prevalent [3, 4] and are usually extensively metabolized [5]. This makes it difficult to know the parent compound which was consumed. For this reason, it is important to study the metabolism of such emerging compounds. Identifying marker metabolites can help Forensic Toxicologists propose which NPS might have been consumed [6].

SC Effects

Cannabinoid psychotropic effects have been found to be mediated through the G-coupled CB_1 and CB_2 receptors [7]. CB_1 receptors are found in neurons of the central nervous system whilst CB_2 receptors are localized in tissues of the immune system [7]. Cannabinoid consumption results in CB_1 receptor mediated inhibition of synaptic transmission [8, 9] which can lead to mood changes, affecting pain perception, temperature regulation, sleep, and the cardiovascular system [10, 11]. This is important because synthetic cannabinoids have been shown to have a high affinity for either the CB_1 or the CB_2 receptors [12, 13] which can prolong the effects on consumers. In a survey of 50 patients conducted by Hermanns-Clausen et al. the duration of symptoms from synthetic cannabinoids lasted from one hour to more than 24 hours [11].

Classes of SCs

SCs were previously classified by structure and were divided into seven major groups: naphthoylindoles (e.g. JWH-018), naphthylmethylindoles (e.g. JWH-175), naphthylmethylindenes (e.g. JWH-176), naphthoylpyrroles (e.g. JWH-307), phenylacetylindoles (e.g. JWH-250), cyclohexylphenols (e.g. CP 47,497), and classical cannabinoids (e.g. HU-210) [14]. An example of each class in comparison to Δ^9-THC is shown in Figure 1. Constant modification of these compounds made this classification system obsolete. Instead of naming SCs after the inventor of the compound, researchers now use key components of the structure. These components include the core, linker, linked group and tail[15] as shown in Figure 2. Code

names can be derived from the chemical names. For example, the code name for N-(1-**a**damantyl)-1-**p**entyl-1H-**i**ndole-3-**ca**rboxamide is APICA.

The SCs used in this study is shown in Figure 2. PX2 has been declared a hazardous or illegal substance in Sweden amongst other countries [16]. PX1 and PX2 were declared dangerous substances by the Louisiana Legislature in 2015, and was based upon the substances high potential for abuse, lack of medical use in the United States, no accepted safety for use under medical supervision, and hazard to the health and safety of the Louisiana residents [17]. The binding affinity of PX1 is 485±117 and 164±17 nM at the CB_1 and CB_2 receptors respectively[18]. The binding affinity of PX2 is 127±43 and 17.4±1.4 nM at the CB_1 and CB_2 receptors respectively[18]. The binding affinity of (S)APP-CHMINACA at the CB_1 receptor is 251 nM and 8.09 nM at the CB_2 receptor with a selective index of 31.0 [19]. Doi *et al* reported the binding affinity of (R)APP-CHMINACA as 33.7 µM and 190 nM at the CB_1 and CB_2 receptors respectively, with a selective index of 68.8 making (S)APP-CHMINACA more potent.

As shown in Figure 2, although similar in structure, PX1 has an indole core whereas PX2 has an indazole core. Similar to PX2, PX3 has an indazole core but a cyclohexylmethyl tail. These differences are enough for each to be categorized separately. The PINACA class has an n-pentyl tail, indazole core, carboxamide linker but varying linked groups. The CHMINACA class has a cyclohexylmethyl tail, indazole core, carboxamide linker but varying linked groups. PICA classes contain an indole core, n-pentyl tail, carboxamide linker and varying linked groups.

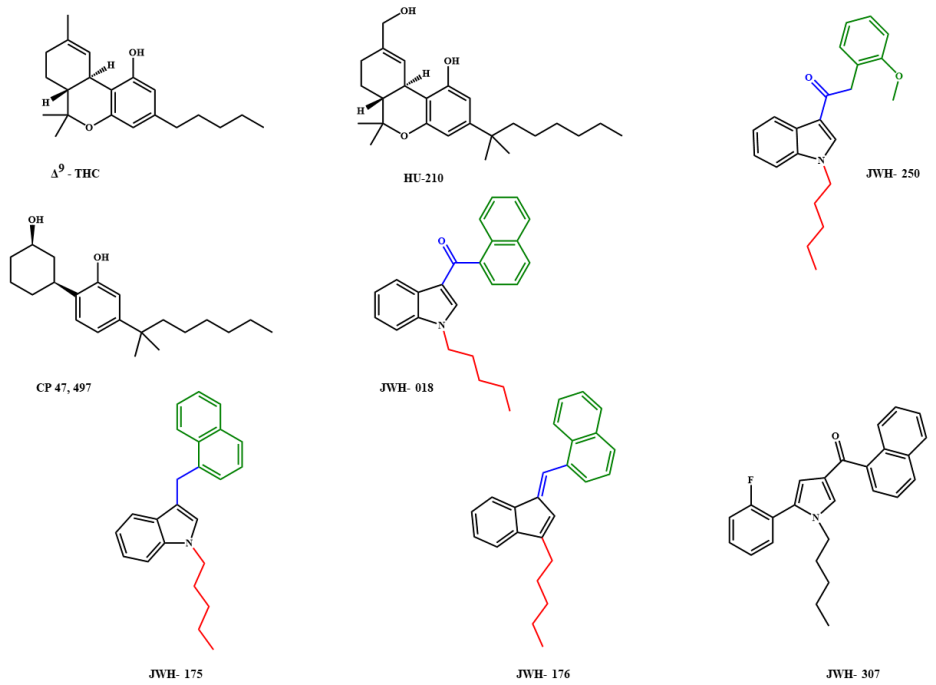

Figure 1: Examples of synthetic cannabinoids in comparison to Δ^9-THC.

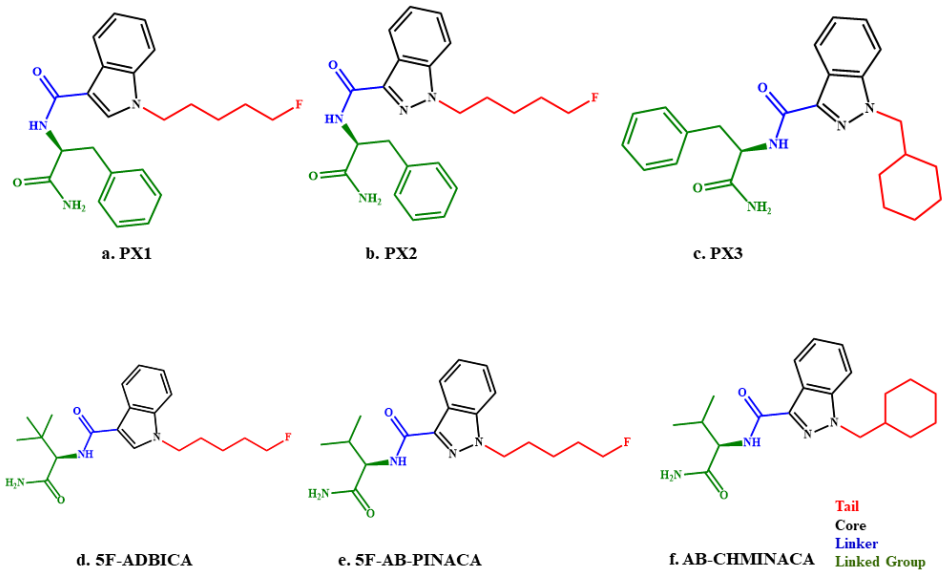

Figure 2: Structures of PX1, PX2, PX3 and their analogue. The analogue pairs are: (a) and (d), (b) and (e), (c) and (f).

Models for Metabolite Identification

In vitro studies which elucidate marker metabolites have been performed using human liver microsomes and hepatocytes [20]. Hepatocytes contain uptake and efflux transporters for the movement of drugs across cell membranes [21] and the necessary enzymes and co-factors for drug metabolism in concentrations similar to the liver, thereby close to *in vivo* conditions [22]. However, they are expensive, not readily available, preparations can only be used once[22, 23], and they have limited viability [24]. Human liver microsomes offer an affordable alternative. It is a well characterized *in vitro* model which retains enzyme activity for many years when frozen at −80℃ [24]. Drug biotransformation and pharmacokinetics data such as half-life and clearance can be derived from microsomal models [25],[26]. The time taken for the concentration of a drug to decrease by half is called its half-life. Intrinsic clearance is the assessment of the liver's activity towards a drug and can be used to confirm metabolism as the major route of drug clearance [27, 28]. Microsomal clearance can be scaled to calculate liver and hepatic clearance thereby increasing understanding of *in vivo* conditions. Although half-life and clearance are important parameters used for drug discovery and dosing regimens, they are equally useful in forensic testing as they can indicate if the parent drug or metabolite is a better proposition for drug consumption. A drug's structure can be useful in determining the extent of metabolism. Studies have shown that lipophilic drugs have greater clearance and therefore undergo extensive first pass metabolism [29–31],[32].

Drug metabolizing enzymes are classified as phase I and phase II. Phase I enzymes consist of the cytochrome P450 (CYP) superfamily of microsomal enzymes found in the liver, lungs, kidneys and gastrointestinal tract [33] and play a crucial role in drug metabolism [34]. Phase II enzymes include sulfotransferases [35], UDP-glucoronosyltransferases, epoxide hydrolases, glutathione S-transferases and N-acetyltransferases among others. Drugs are generally conjugated during phase II metabolism and are made more hydrophilic to enhance excretion in urine [33]. During phase I, drugs are modified through hydrolysis, oxidation, and reduction [20] therefore enabling further conjugation during phase II. Although microsomes lack phase II enzymes, they are rich in cytochrome P450 (CYP) enzymes [36],[37],[38]. This enables the detection of metabolites prior conjugation in phase II.

In silico studies may be conducted to predict metabolites of uncharacterized novel psychoactive substances. A knowledge of the solubility of the drug can help predict how it

interacts with other molecules in a particular environment and therefore the transformations it may undergo [39]. In this study Compound Discoverer® was used to elucidate metabolism mainly through phase I metabolism due to the limited phase II enzymes present in liver microsomes.

Materials and Methods

PX-1, PX-2, PX-3, NM2201, 5FPB22 metabolite, PB-22-d_9, standards purchased from Cayman Chemical Company® (Ann Arbor, Michigan). NADPH Regenerating System solution A and B, and 0.5 M potassium phosphate buffer, pH 7.4 purchased from Corning® (Woburn, MA). HPLC grade methanol, acetonitrile with 0.1% formic acid as solvent B and water in 0.1% formic acid as solvent A purchased from Fisher Chemical® (Fair Lawn, New Jersey). Thermo Scientific Hypersil GOLD C18 column (30 mm x 2.1 mm x 3 μm), guard column holder and 5 μm drop-in guard cartridges, human liver microsomes (20 mg/mL) purchased from Thermo Scientific®.

Method Validation

Bias, calibration, carryover, ionization suppression and enhancement, precision were evaluated using SWGTOX guidelines [40]. Limit of detection was estimated using equation 1.

$$LOD = \frac{(\overline{X_{noise}} + 3 * SD_{noise}) * C_1}{Signal} \quad \textbf{(1)}$$

All compounds were optimized and analyzed on an Agilent 6470A Triple Quadrupole LC/MS (Agilent Technologies) coupled with a 1290 Infinity II LC system (Agilent Technologies). The method parameters are listed in Supplementary Table 1 (Appendix 1) and the transitions in Table 1. The cell accelerator voltage was 4 V. The calibrators included 5.0, 10.0, 25.0, 50.0, and 100.0 ng/mL and were prepared in blank matrix which comprised of 0.5 M potassium phosphate buffer pH 7.4, deionized water, and acetonitrile. The low, medium and high controls were 10.0 ng/mL, 50.0 ng/mL and 100.0 ng/mL respectively. Each sample was spiked with 25.0 ng/mL PB22-d_9 internal standard.

Table 1: Compound transitions.

Compound	Precursor Ion	Product Ion	Frag (V)	CE (V)
5FPB22 met	250.1	206.2	90	15
		132.1	90	25
		118.1	90	25
NM2201	376.2	232.0	55	12
		144.0	55	48
		115.9	55	72
$PB22d_9$	368.2	223.1	68	12
		145.0	68	48
		117.0	68	72
PX-1	396.2	232.0	70	20
		144.0	70	52
		116.0	70	76
PX-2	397.2	233.0	75	24
		213.0	75	40
		145.0	75	50
PX-3	405.2	360.1	85	16
		241.0	85	28
		145.0	85	48

Metabolite Identification

Microsome incubation procedure was adapted from previous studies[41]. The HLM suspension was thawed at 37℃. The reaction mixture contained 780 μL distilled water, 100 μL 0.5 M potassium phosphate buffer pH 7.4, 10 μL solution B, 10 μL 100.0 μmol/L drug, 50 μL HLM suspension, and 50 μL solution A to initiate the reaction. NM2201 was used as a positive control and the metabolite1-(5-fluoropentyl)-1H-indole-3-carboxylic acid (5FPB22) was monitored as previously studied [42]. All samples were incubated at 37℃. Aliquots of 500 μL were collected at 0, and 60 minutes and was quenched with 500 μL ice-cold acetonitrile. The samples were centrifuged at 10,000 rpm for 5 minutes. The supernatant was dried under nitrogen gas at 50℃ and reconstituted with 300 μL methanol and acetonitrile (50:50). Samples were analyzed using a Q Exactive Hybrid Quadrupole-Orbitrap mass spectrometer (ThermoFisher Scientific®) coupled with a PAL HTC Accelera autosampler and Accelera 1250 pump. The gradient system was as follows: 10% B until 0.6 minutes and held until 10.5 minutes, ramped to 95% B and held until 11.0 minutes, ramped down to 10% B and held until 13.0 minutes. The flow rate was 500 µL/min.

Data was acquired using Full MS and $ddMS^2$ using the optimized parameters in Table 2. Compound Discoverer v2.1.0.401 (ThermoFisher Scientific®) was used for elucidation of metabolite profiling and Thermo XCalibur™ v2.2 (ThermoFisher Scientific®) to verify mass

spectra. The workflow from Compound Discoverer is shown in Appendix 1. The phase I transformations for NM2201, PX-1 and PX-2 included dehydration, desaturation, hydration, nitro reduction, oxidation, oxidative deamination to alcohol and ketone, oxidative defluorination, reduction, and reductive defluorination whereas no fluorine transformations were selected for PX-3 as it has no fluorine in its structure. Glucuronide conjugation was the only phase II transformation assessed. Dealkylation and dearylation were applied for a maximum of two steps utilizing a minimum mass of 150 Da. Mass tolerance was set to 5 ppm. The experiment was duplicated.

Table 2: Q- Exactive Full MS/ dd-MS^2 properties used for metabolite identification.

General	
Runtime	0 to 13 min
Polarity	positive
Default charge	2
Full MS	
Resolution	70,000
AGC target	1e6
Maximum IT	200 ms
Scan range	100 to 600 *m/z*
dd-MS^2/ dd-SIM	
Resolution	35,000
AGC target	1e5
Maximum IT	50 ms
Loop count	5
TopN	5
Isolation window	2.0 *m/z*
(N)CE/ stepped nce	35
dd Settings	
Minimum AGC target	1e3
Intensity threshold	2e4
Exclude isotope	on
Dynamic exclusion	10.0 s

Metabolic Stability using HLM

The incubation procedure was similar to the metabolite identification procedure described above but aliquots of 100 μL were collected at 0, 3, 8, 13, 20, 45, and 60 minutes after the reaction has been initiated. The supernatant was spiked with 10 μL of 25 ng/mL internal standard and analyzed using dynamic MRM on an Agilent 6470A Triple Quadrupole LC/MS (Agilent Technologies) coupled with a 1290 Infinity II LC system (Agilent Technologies). A linear gradient elution was used (Supplementary Table 1). Sample volume injected was 2 μL. The

autosampler temperature was kept at 5℃. The gas temperature set to 325℃; gas flow to 5 L/min; nebulizer to 45 psi; sheath gas temperature to 350℃; sheath gas flow to 11 L/min; capillary voltage to 3500 V; and nozzle voltage to 500 V.

Data analysis performed using MassHunter B.08.00 (Agilent Technologies). The quantitative transitions were 250.1→ 206.2, 376.2→ 232.0, 368.2→ 223.1, 396.2→ 232.0, 397.2→ 233.0, 405.2→ 241.0 for 5FPB22 metabolite, NM2201, $PB22_9$, PX-1, PX-2 and PX-3 respectively. Optimization parameters for each compound is shown in Table 1. Half-life and clearance were determined from six replicates.

Results and Discussion

Method Validation

Bias was less than ±20% for all compounds. All analytes were within ±20% ionization suppression/enhancement at 25.0 ng/mL and 100.0 ng/mL except 5FPB22 metabolite which was 27% at low range and 23% at the high range. This was acceptable as 5FPB22 metabolite was used qualitatively. The correlation coefficient for within and between injection variability were 0.999 and 1.000 for all analytes respectively. Between-run and within-run %CV were within ±10%. The estimated LOD was 0.4, 0.6, 0.3, 0.3, and 1.8 ppb for PX-1, PX-2, PX-3, NM2201, and 5FPB22 metabolite respectively. No carryover was observed.

Metabolic Stability

Clearance was determined using the natural logarithm of the drug/ internal standard ratio. Equation 2 was used to calculate half-life values. *k* was calculated from the slope of the time vs LN (drug/ internal standard) ratio. Clearance was calculated using equation 3 adapted from previous literature [27].

$$T_{\frac{1}{2}} = \frac{\mathrm{LN}(2)}{\mathrm{k}} \quad \textbf{(2)}$$

$$CL_{int} = k(min^{-1})\frac{[V]_{incubation}(mL)}{[P]_{incubation}(mg)} = \frac{ln2}{t_{\frac{1}{2}}(min)}\frac{[V]_{incubation}(mL)}{[P]_{incubation}(mg)} \quad \textbf{(3)}$$

$$\Rightarrow (mL/min\,mg)$$

where [V] is the incubation volume in *mL* and [P] is the amount of microsomal protein in the incubation. Table 3 summarizes the half-life and clearance data. The half-life of the control, naphthalen-1-yl 1-(5-fluoropentyl)-1H-indole-3-carboxylate (NM2201) was 6.7 ± 0.75 minutes and intrinsic clearance, 0.103 mL/min/mg. Diao *et al* reported a half-life value of 8.0 ± 1.5 minutes and *in vitro* clearance as 0.088 mL/min/mg for NM2201 [42]. The calculated half-lives for PX-1, PX-2 and PX-3 were 15.1 ± 1.02, 3.4 ± 0.27, and 5.2 ± 0.89 respectively as shown in Table 3. Plots of the half-life data is shown in Appendix 1. PX-1 showed the lowest clearance rate, 0.046 mL/min/mg whereas PX-2 had the highest clearance rate, 0.202 mL/min/mg. Drugs may be excreted in urine unchanged or chemically modified to facilitate excretion. In this study, a higher clearance rate was expected for the more polar PX-1 but the lack of phase II enzymes

may have limited clearance. PX-2 and PX-1 were expected to have comparable clearance rates due to structural similarities. The difference in the observed values may have been due to an extra nitrogen atom in PX-2 which made it less polar, but sufficiently metabolized by CYP450 enzymes to facilitate excretion. However, the results indicate that the SCs are all extensively metabolized.

A survey of the literature yielded binding affinities, clearance and half- life data for SCs structurally similar to the ones investigated in this study (Table 3). In this study, PX-1, PX-2 and PX-3 were compared to other PICA, PINACA and CHMINACA SCs respectively, where the only difference was the linked group. Although there is limited half-life and clearance data, PX-1 showed the lowest clearance rate in the PICA class and was the least potent based on K_i values. It is possible the phenylalaninamide component of PX-1 increases its polarity more than 5F-CUMYLPICA and STS-135 which require higher clearance. However, further investigations for amide containing PICA SCs such as 5F-ADBICA, 5F-AB-PICA and 5F-SDB-006 are required to support these observations. Although PX-2 is the least potent PINACA, it is not the least cleared. A similar trend to PX-1 is expected but would require further investigations. No data was available for other CHMINACA SCs, but low polarity compounds may show higher clearance *in vitro*. A class comparison of half-life and clearance data can provide useful information about emerging compounds in that class.

Table 3: Half-life, clearance and K_i summary for selective SC structurally related to PX-1, PX-2, PX-3.

Drug	$T_{\frac{1}{2}}$ (mins)	$Cl_{int,micr}$ (mL/min/mg)	K_i at CB_1 (nM)	K_i at CB_2 (nM)
PICA				
5F-CUMYL-PICA	1.77[43]	0.39[43]	1.37 ± 0.26[18]	29.1 ± 2.4[18]
STS-135	3.1 ± 0.2[44]	0.222[44]	2.51 ± 0.35[45]	0.794 ± 0.071[45]
5F-ADBICA	N/A	N/A	2.72 ± 0.35[18]	1.83 ± 0.11[18]
5F-MDMB-PICA	N/A	N/A	9.35 ± 0.07[46]	8.13 ± 0.05[46]
5F-MMB-PICA	N/A	N/A	15.2 ± 5.0[18]	19.8 ± 4.2[18]
5F-AB-PICA	N/A	N/A	35 ± 7.7[18]	89.0 ± 33.2[18]
5F-SDB-006	N/A	N/A	71.9 ± 13.5[45]	430 ± 73[45]
PX-1 (APP-PICA)	15.1 ± 1.02	0.046	485 ± 117[18]	164 ± 17[18]
PINACA				
5F-AMB	1.0 ± 0.2[47]	0.67[47]	1.13 ± 0.48[18]	1.38 ± 0.22[18]
5F-ADB-PINACA	N/A	N/A	1.43 ± 0.69[18]	0.694 ± 0.078[18]
5F-APINACA	N/A	N/A	1.94 ± 0.55[45]	0.266 ± 0.041[45]
5F-AB-PINACA	35.9 ± 3.0[48]	0.019[48]	4.96 ± 1.37[18]	3.77 ± 0.25[18]
5F-ADB	N/A	N/A	23.3 ± 10.2[18]	5.99 ± 2.47[18]
PX-2 (APP-PINACA)	3.4 ± 0.27	0.202	127 ± 43[18]	17.4 ± 1.4[18]
CHMINACA				
MDMB-CHMINACA	N/A	N/A	0.135 ± 0.028[18]	0.222 ± 0.034[18]
MAB-CHMINACA	N/A	N/A	0.333 ± 0.059[18]	0.331 ± 0.048[18]
MA-CHMINACA	N/A	N/A	0.339 ± 0.073[18]	0.301 ± 0.092[18]
AB-CHMINACA	N/A	N/A	1.72 ± 0.14[18]	1.91 ± 0.20[18]
			0.78 ± 0.11[49]	0.45 ± 0.03[49]
PX-3 (APP-CHMINACA)	5.2 ± 0.89	0.133	(R) 33.7 µM[19]	(R) 190[19]
			(S) 251[19]	(S) 8.09[19]
			9.81 ± 4.56[18]	4.39 ± 0.59[18]

Metabolite Identification

PX-1 Metabolic Pathway

The four proposed phase I metabolites of PX-1 in this study, are shown in Figure 3. Oxidation was the common route of biotransformation for all PX-1 metabolites. SRF-3 ((1-(5-fluoropentyl)-1H-indole-3-carbonyl)phenylalanine), was the only fluorinated metabolite detected and eluted later than PX-1 despite containing more oxygen atoms. Although metabolites are usually more hydrophilic than parent compounds to facilitate excretion, in this study less polar metabolites were observed possibly because phase II enzymes were lacking. The clearance rate of PX-1 suggest conjugation as a dominant biotransformation pathway. A summary of the retention times and diagnostic ions is shown in Table 4 and chromatograms are shown in Appendix 1.

As shown in Figure 4, the base peak from SRF-1 and SRF-4 at *m/z* 230.1180 is a loss of phenylalaninamide ($C_9H_{12}N_2O$, 164.0949 Da) and phenylalanine ($C_9H_{11}NO_2$, 165.0793 Da) respectively. A similar loss for PX-1 and SRF-3 showed the same characteristic ion at *m/z* 232.1137 ± 0.0001 because they contain fluorine. PX-1 and its metabolites all yielded the characteristic ion at *m/z* 144.0446 ± 0.0002 which corresponds to a loss of either the fluoropentyl (C_5H_9F) or hydroxypentyl ($C_5H_{10}O$) chain from the base peak.

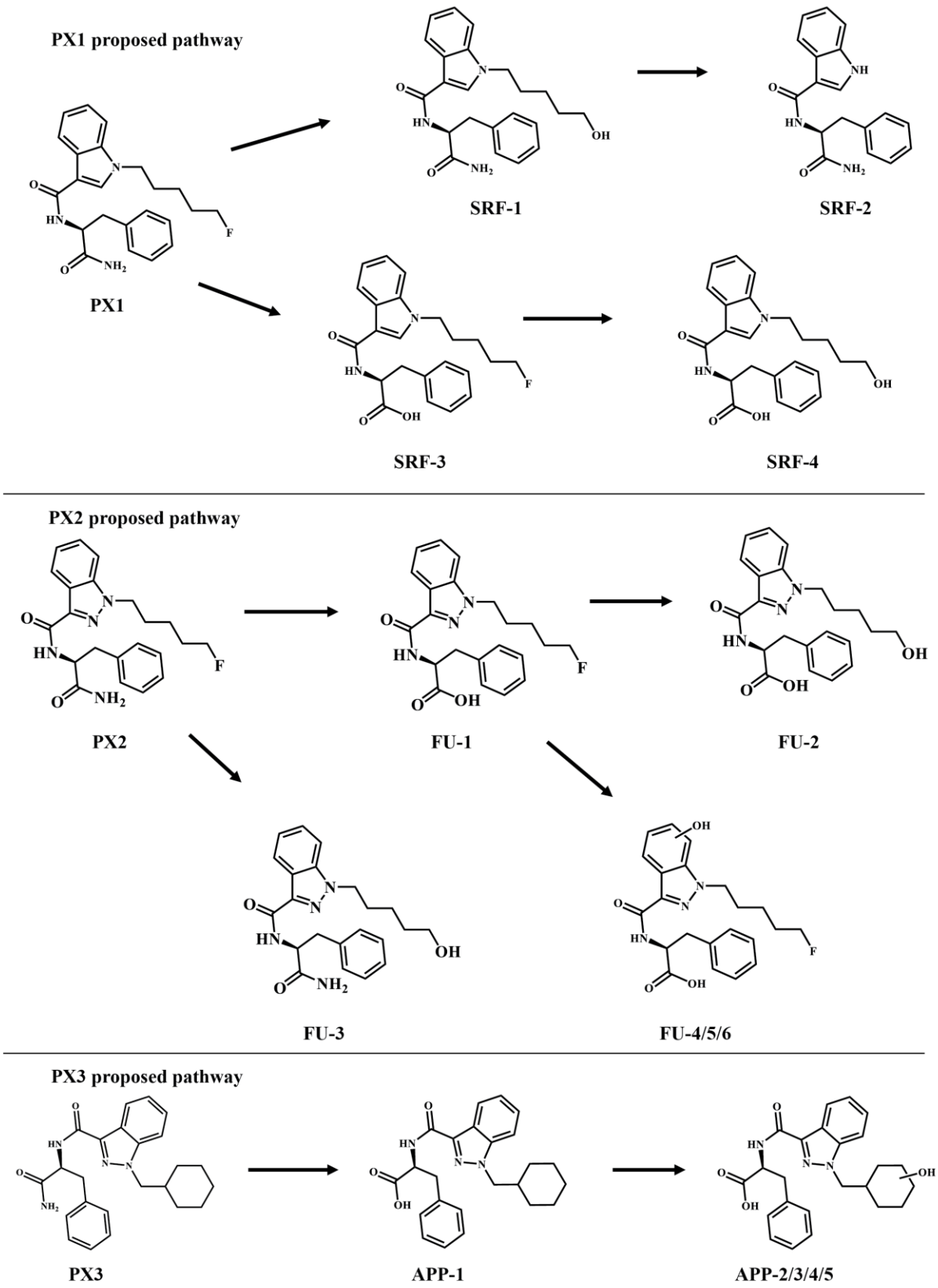

Figure 3: Structural elucidation of metabolites for PX-1, PX-2 and PX-3.

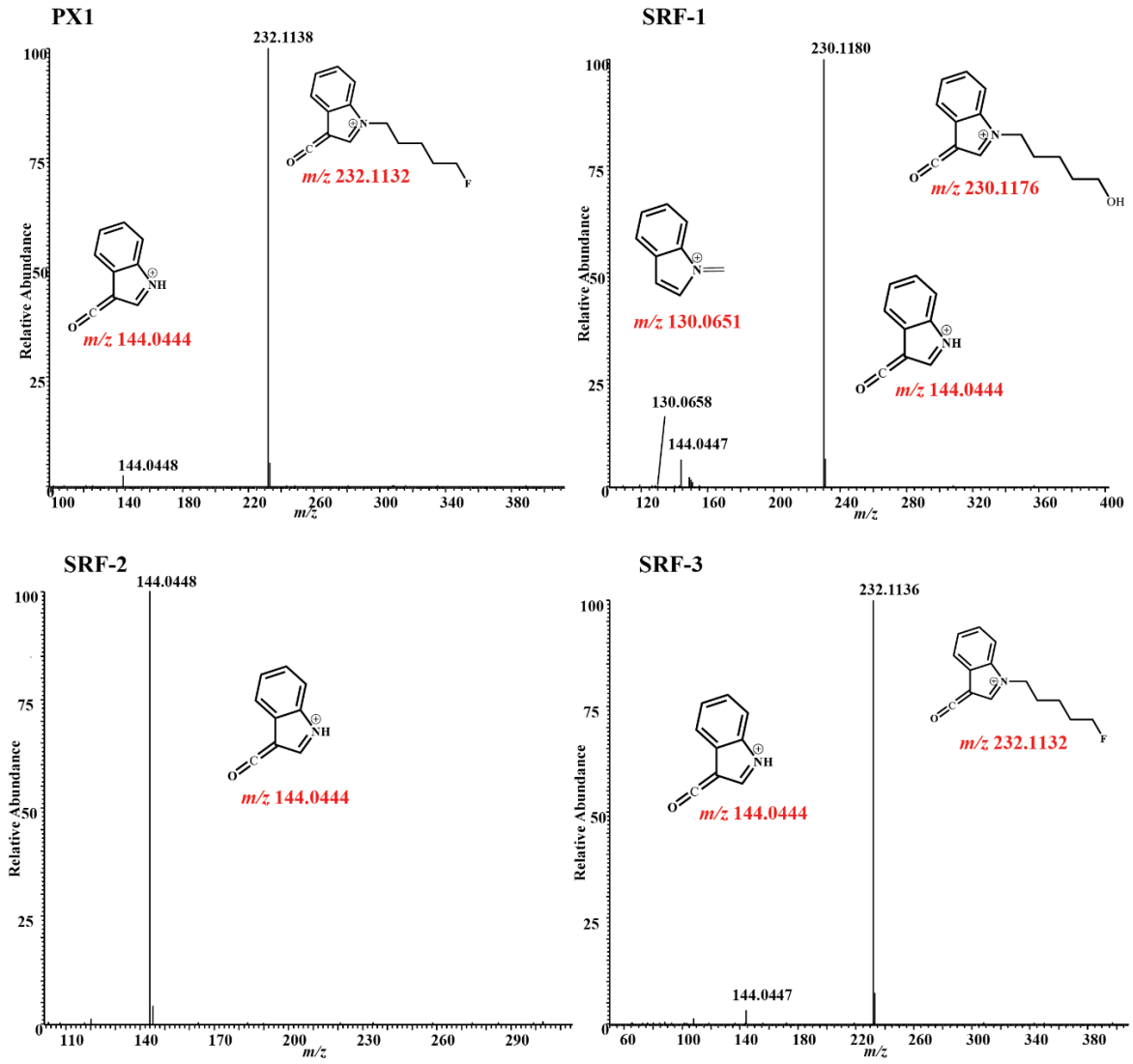

Figure 4: MS/MS spectra of PX-1 and proposed metabolites.

Table 4 : PX-1 metabolite identification summary.

Compound	Transformation	RT (min)	$[M+H]^+$	Mass Error (ppm)	Diagnostic Ions	Peak Area	Rank
PX-1 (parent)	---	5.59	396.2091	-2.3	232.1138, 144.0448	2.62e5	---
SRF-1	Oxidative defluorination	4.41	394.2129	-1.0	230.1180, 144.0447, 130.0658	1.22e6	1
SRF-2	Dehydration, reduction	3.98	308.1393	-1.9	144.0448	6.96e5	2
SRF-3	Oxidative deamination to alcohol	6.05	397.1928	-1.5	232.1136, 144.0444	2.46e5	3
SRF-4	Oxidative deamination to alcohol, oxidative defluorination	4.81	395.1973	-2.0	230.1180, 144.0444	1.06e5	4

PX-2 Metabolic Pathway

Figure 3 shows six proposed metabolites of PX-2 from this study. Oxidation was the major route of biotransformation. Four fluorinated metabolites FU-1 ((1-(5-fluoropentyl)-1H-indazole-3-carbonyl)phenylalanine), 4, 5 and 6 were observed but FU-4/5/6 eluted before FU-1 due to the presence of the extra hydroxyl group on the indazole core, as confirmed by the retention times in Table 5. Chromatograms of PX-2 and metabolites are shown in Appendix 1.

PX-2 and the major metabolite FU-1 shared the same diagnostic ions as shown in Figure 5. Although a fragmentation pattern similar to PX-1 was expected, the possible rearrangement of PX-2 and FU-1 resulted in the base peak at *m/z* 251.1194. The diagnostic ion at *m/z* 233.1088 ± 0.0001, common to PX-2, FU-1, FU-5 and FU-6 is consistent with the loss of phenylalaninamide or phenylalanine in addition to the loss of OH for FU-5 and FU-6. The characteristic ion at *m/z* 213.1025 ± 0.0002 which corresponds to $C_{13}H_{13}N_2O^+$, was common to all metabolites of PX-2 but FU-4. Another commonly observed characteristic ion was *m/z* 145.0399 ± 0.0001 ($C_8H_5N_2O^+$).

The hydroxylation of FU-1 on the indazole core resulted in the isomer metabolites FU-4, FU-5, and FU-6 with molecular ion *m/z* 414.1829. The characteristic ion at *m/z* 267.1143 ± 0.0001 is a possible rearrangement of the phenyl methyl group on the indazole core. The ion at *m/z* 249.1037 ($C_{13}H_{14}FN_2O_2^+$) for FU-4 (Figure 5) indicates the hydroxyl group is on the indazole core and is supported by the subsequent secondary ion at *m/z* 175.0506 ($C_9H_7N_2O_2^+$).

Additional evidence is provided by the observation of fragments at *m/z* 161.0348 ($C_8H_5N_2O_2^+$) and *m/z* 229.0975 ($C_{13}H_{13}N_2O_2^+$). However, confirmation of the proposed metabolites would require standards which were not available.

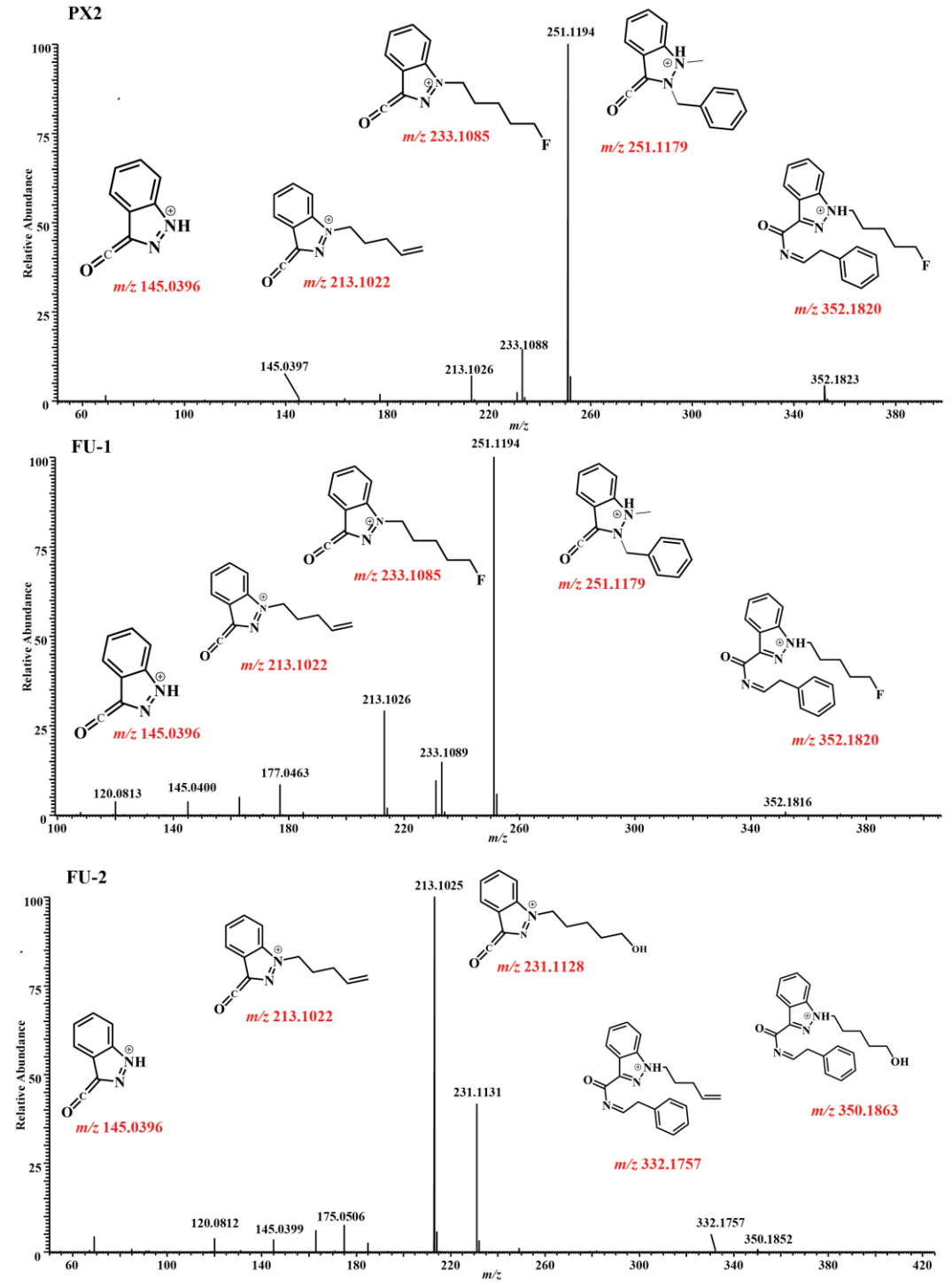

Figure 5: MS/MS spectra of PX-2 and proposed metabolites.

Table 5: PX-2 metabolite identification summary.

Compound	Transformation	RT (min)	$[M+H]^+$	Mass Error (ppm)	Diagnostic Ions	Peak Area	Rank
PX-2 (parent)	---	5.76	397.2038	-1.0	352.1823, 251.1194, 233.1088, 213.1026, 145.0397	1.49e8	---
FU-1	Oxidative deamination to alcohol	6.31	398.1884	-2.5	352.1816, 251.1194, 233.1089, 213.1026, 145.0400	5.95e8	1
FU-2	Oxidative deamination to alcohol, oxidative defluorination	4.96	396.1921	-0.8	350.1852, 332.1757, 231.1131, 213.1025, 145.0399	1.10e8	2
FU-3	Dehydration, reductive defluorination	4.49	395.2082	-1.0	350.1865, 231.1131, 213.1025	2.73e7	3
FU-4	Dehydration, oxidative deamination to alcohol	4.98	414.1829	-1.2	368.1776, 267.1144, 249.1037, 175.0506, 145.0399	2.25e7	4
FU-5	Dehydration, oxidative deamination to alcohol	5.65	414.1829	-1.2	267.1143, 251.1193, 249.1038, 233.1089, 229.0975, 213.1026, 161.0348	8.43e6	5
FU-6	Dehydration, oxidative deamination to alcohol	5.30	414.1829	-1.2	267.1142, 251.1193, 233.1087, 213.1022, 145.0400	4.67e6	6

PX-3 Metabolic Pathway

Figure 3 shows five detected metabolites of PX-3. The major metabolite APP-1 ((1-(cyclohexylmethyl)-1H-indazole-3-carbonyl)phenylalanine), was formed from the deamination of PX-3. Unlike PX-1 and PX-2, fluorine is absent in PX-3 but the cyclohexyl methyl group has a similar effect on its hydrophilicity. As shown by the retention times in Table 6, APP-1 was least polar whereas the hydroxylated metabolites eluted first. Appendix 1 shows the chromatogram of PX-3 and metabolites.

PX-3 and APP-1, have similar MS/MS spectra. The diagnostic ion m/z 360.2073 for PX-3, shown in Figure 6 is a loss of CH_3NO, 45.0220 Da whereas the same ion is a loss of CH_3O_2, 46.0057 Da for APP-1. The base peak *m/z* 241.1340 for both compounds resulted from the loss of phenylalaninamide and phenylalanine for PX-3 and APP-1 respectively. Subsequent loss of methylenecyclohexane, C_7H_{12}, 96.0939 Da resulted in *m/z* 145.0399 also observed in metabolites of PX-2. A noteworthy fragment, *m/z* 259.1444 differs from *m/z* 360.2077 by 101.0633 Da and from *m/z* 241.1338 by 18.0106 Da. Analysis of standards would help explain these observations.

The minor metabolites APP-2/3/4/5 ((1-((hydroxycyclohexylmethyl)methyl)-1H-indazole-3-carbonyl)phenylalanine) are isomers which came from the hydroxylation of cyclohexane on APP-1. Figure 6 shows the observed MS/MS spectrum was the same for each isomer. Diagnostic ion *m/z* 404.1974 is from the dehydration of molecular ion *m/z* 422.2081. Subsequent loss of CH_2O_2, 46.0061 Da resulted in *m/z* 358.1913. Loss of phenylalanine, 165.0793 Da from the molecular ion resulted in the base peak, *m/z* 257.1288. Subsequent dehydration resulted in *m/z* 239.1179.

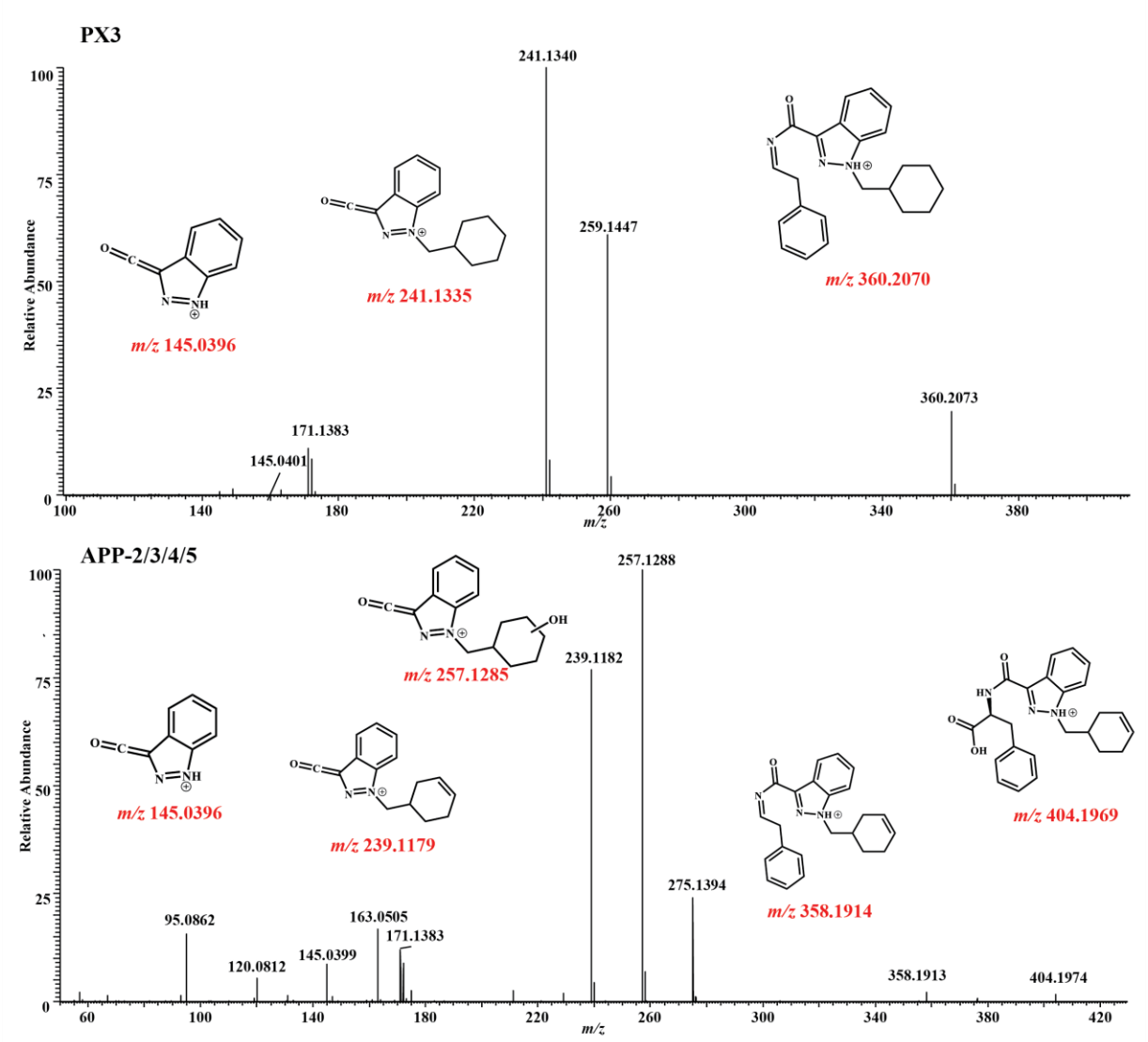

Figure 6: MS/MS spectra of PX-3 and proposed metabolites.

Table 6: PX-3 metabolite identification summary.

Compound	Transformation	RT (min)	$[M+H]^+$	Mass Error (ppm)	Diagnostic Ions	Peak Area	Rank
PX-3 (parent)	---	6.89	405.2293	-2.0	360.2073, 241.1340, 145.0401	3.23e8	---
APP-1	Oxidative deamination to alcohol	7.47	406.2134	-2.2	360.2077, 241.1338, 145.0399	7.26e8	1
APP-2	Dehydration, oxidative deamination to alcohol	5.03	422.2081	-1.7	404.1974, 358.1913, 257.1288, 239.1182, 145.0396	2.29e8	2
APP-3	Dehydration, oxidative deamination to alcohol	5.17	422.2081	-1.7	404.1974, 358.1913, 257.1288, 239.1182, 145.0396	4.97e7	3
APP-4	Dehydration, oxidative deamination to alcohol	5.88	422.2081	-1.7	404.1974, 358.1913, 257.1288, 239.1182, 145.0396	2.53e7	4
APP-5	Dehydration, oxidative deamination to alcohol	5.38	422.2081	-1.7	404.1974, 358.1913, 257.1288, 239.1182, 145.0396	2.35e7	5

Suggested marker metabolites

SRF-1 can be considered a marker metabolite because it was the most abundant PX-1 metabolite and is sufficiently polar. SRF-2, the second most abundant metabolite of PX-1 is a good target because it was the most polar of the detected metabolites. FU-1 and APP-1 were the major metabolites of PX-2 and PX-3 respectively, and while good marker metabolites further transformation may occur to increase elimination. FU-2 and APP-2 are also likely marker metabolites which may be detected in urine. The detected metabolites for the targeted compounds did not overlap with each other's proposed metabolic pathway or previously characterized SCs of the same class. However, similarities in diagnostic ions were observed. Two common fragments *m/z* 144 and *m/z* 232 observed in PX-1 and similar PICA SCs are characteristic of the indole core and fluoropentyl tail [43, 44, 50]. The fragments *m/z* 145, 233, and 213 were observed in the elucidation of PX-2 and other PINACA compounds and are

characteristic of the indazole core and fluoropentyl tail [47, 48, 51, 52]. The most common fragments *m/*z 145, 257, and 241 observed in PX-3 and other CHMINACA SCs are characteristic of the indazole core and cyclohexylmethyl tail. These observations suggest fragments corresponding to the core of SCs may be insufficient for confirmation and therefore require fragments with the core and parts of the tail or linked group.

Conclusion

Potent synthetic cannabinoids are constantly emerging on the black market. Studies have shown these substances to undergo extensive biotransformation thus making parent compounds challenging to detect by existing methods. However, *in vitro* studies are useful in identifying potential marker metabolites.

The observations in this study suggest the metabolic pathways of PX-1, PX-2 and PX-3 do not overlap. Four, six, and five metabolites of PX-1, PX-2 and PX-3 respectively, were detected and their structures elucidated. Oxidation was the common biotransformation between compounds and the major metabolite of PX-1 was transformed through oxidative defluorination whereas PX-2 and PX-3, through oxidative deamination. SRF-1, SRF-2, FU-1, FU-2, APP-1 and APP-2 are promising marker metabolites. This work showed PX-1 had the highest half-life (15.1 ± 1.02 mins) and subsequently the lowest clearance (0.046 mL/min/mg) whereas PX-2 had the highest clearance (0.202 mL/min/mg). Comparison of available clearance data for similar compounds indicate functional groups which reduce polarity have higher clearance rates, but further research is required to support this hypothesis. Standards for marker metabolites and *in vivo* studies can confirm observations in this study and could therefore include the metabolites in toxicology screens.

References

1. Gurney SMR, Scott KS, Kacinko SL, Presley BC, Logan BK (2014) Pharmacology, Toxicology, and Adverse Effects of Synthetic Cannabinoid Drugs. Forensic Sci Rev 26:53–78

2. EMCDDA. European drug report 2015: trends and developments.

3. Adamowicz P, Gieroń J, Gil D, Lechowicz W, Skulska A, Tokarczyk B (2016) The prevalence of new psychoactive substances in biological material--a three-year review of casework in Poland. Drug Test Anal 8:63–70

4. Khaled SM, Hughes E, Bressington D, Zolezzi M, Radwan A, Badnapurkar A, Gray R (2016) The prevalence of novel psychoactive substances (NPS) use in non-clinical populations: a systematic review protocol. Syst Rev 5:195. https://doi.org/10.1186/s13643-016-0375-5

5. Diao X, Scheidweiler KB, Wohlfarth A, Pang S, Kronstrand R, Huestis MA (2016) In Vitro and In Vivo Human Metabolism of Synthetic Cannabinoids FDU-PB-22 and FUB-PB-22. AAPS J 18:455–464. https://doi.org/10.1208/s12248-016-9867-4

6. Castaneto MS, Wohlfarth A, Desrosiers NA, Hartman RL, Gorelick DA, Huestis MA (2015) Synthetic cannabinoids pharmacokinetics and detection methods in biological matrices. Drug Metab Rev 47:124–174. https://doi.org/10.3109/03602532.2015.1029635

7. Pertwee RG, Howlett AC, Abood ME, Alexander SPH, Di Marzo V, Elphick MR, Greasley PJ, et al (2010) International Union of Basic and Clinical Pharmacology. LXXIX. Cannabinoid Receptors and Their Ligands: Beyond CB1 and CB2. Pharmacol Rev 62:588–631. https://doi.org/10.1124/pr.110.003004

8. Szabo B, Schlicker E (2005) Effects of Cannabinoids on Neurotransmission. In: Pertwee RG (ed) Cannabinoids. Springer Berlin Heidelberg, Berlin, Heidelberg, pp 327–365

9. Pertwee RG (2008) Ligands that target cannabinoid receptors in the brain: from THC to anandamide and beyond. Addict Biol 13:147–159. https://doi.org/10.1111/j.1369-1600.2008.00108.x

10. Murray RM, Morrison PD, Henquet C, Forti M Di (2007) Cannabis, the mind and society:

the hash realities. Nat Rev Neurosci 8:885

11. Hermanns-Clausen M, Kneisel S, Szabo B, Auwärter V (2013) Acute toxicity due to the confirmed consumption of synthetic cannabinoids: clinical and laboratory findings. Addiction 108:534–544. https://doi.org/10.1111/j.1360-0443.2012.04078.x

12. Huffman JW (2009) Cannabimimetic Indoles, Pyrroles, and Indenes: Structure--Activity Relationships and Receptor Interactions. In: Reggio PH (ed) The Cannabinoid Receptors. Humana Press, Totowa, NJ, pp 49–94

13. Simões SS, Silva I, Ajenjo AC, Dias MJ (2014) Validation and application of an UPLC–MS/MS method for the quantification of synthetic cannabinoids in urine samples and analysis of seized materials from the Portuguese market. Forensic Sci Int 243:117–125. https://doi.org/https://doi.org/10.1016/j.forsciint.2014.07.022

14. EMCDDA Synthetic cannabinoids and “Spice” drug profile

15. EMCDDA Synthetic cannabinoids in Europe

16. Agency SPH (2014) Cannabinoids are suggested to be classified as a health hazard

17. (2015) Louisiana Department of Health Notice of Intent

18. Schoeder CT, Hess C, Madea B, Meiler J, Müller CE (2018) Pharmacological evaluation of new constituents of ``Spice'': synthetic cannabinoids based on indole, indazole, benzimidazole and carbazole scaffolds. Forensic Toxicol 36:385–403. https://doi.org/10.1007/s11419-018-0415-z

19. Doi T, Tagami T, Takeda A, Asada A, Sawabe Y (2018) Evaluation of carboxamide-type synthetic cannabinoids as CB1/CB2 receptor agonists: difference between the enantiomers. Forensic Toxicol 36:51–60. https://doi.org/10.1007/s11419-017-0378-5

20. Jia L, Liu X (2007) The conduct of drug metabolism studies considered good practice (II): in vitro experiments. Curr Drug Metab 8:822–829

21. SHITARA Y, LI AP, KATO Y, LU C, ITO K, ITOH T, SUGIYAMA Y (2003) Function of Uptake Transporters for Taurocholate and Estradiol 17β-D-Glucuronide in Cryopreserved Human Hepatocytes. Drug Metab Pharmacokinet 18:33–41.

https://doi.org/10.2133/dmpk.18.33

22. Li AP, Lu C, Brent JA, Pham C, Fackett A, Ruegg CE, Silber PM (1999) Cryopreserved human hepatocytes: characterization of drug-metabolizing activities and applications in higher throughput screening assays for hepatotoxicity, metabolic stability, and drug–drug interaction potential. Chem Biol Interact 121:17–35. https://doi.org/https://doi.org/10.1016/S0009-2797(99)00088-5

23. Ruegg CE, Silber PM, Mughal RA, Ismail J, Lu C, Bode DC, Li A (1997) Cytochrome-P450 induction and conjugated metabolism in primary human hepatocytes after cryopreservation. Vitr Toxicol J Mol Cell Toxicol 10:217–222

24. Zhang D, Luo G, Ding X, Lu C (2012) Preclinical experimental models of drug metabolism and disposition in drug discovery and development. Acta Pharm Sin B 2:549–561. https://doi.org/https://doi.org/10.1016/j.apsb.2012.10.004

25. Obach RS (2001) The prediction of human clearance from hepatic microsomal metabolism data. Curr Opin Drug Discov Devel 4:36—44

26. Houston JB, Carlile DJ (1997) Prediction of Hepatic Clearance from Microsomes, Hepatocytes, and Liver Slices. Drug Metab Rev 29:891–922. https://doi.org/10.3109/03602539709002237

27. Baranczewski P, Stanczak A, Sundberg K, Svensson R, Wallin A, Jansson J, Garberg P, et al (2006) Introduction to in vitro estimation of metabolic stability and drug interactions of new chemical entities in drug discovery and development. Pharmacol Rep 58:453–472

28. Lu C, Li P, Gallegos R, Uttamsingh V, Xia CQ, Miwa GT, Balani SK, et al (2006) Comparison of Intrinsic Clearance in Liver Microsomes and Hepatocytes from Rats and Humans: Evaluation of Free Fraction and Uptake in Hepatocytes. Drug Metab Dispos 34:1600–1605. https://doi.org/10.1124/dmd.106.010793

29. Lin JH, Lu AYH (1997) Role of Pharmacokinetics and Metabolism in Drug Discovery and Development. Pharmacol Rev 49:403–449

30. Toon S, Rowland M (1983) Structure-pharmacokinetic relationships among the barbiturates in the rat. J Pharmacol Exp Ther 225:752–763

31. Xiao JF, Zhou B, Ressom HW (2012) Metabolite identification and quantitation in LC-MS/MS-based metabolomics. TrAC Trends Anal Chem 32:1–14. https://doi.org/https://doi.org/10.1016/j.trac.2011.08.009

32. Seydel JK, Schaper KJ (1986) Quantitative structure-pharmacokinetic relationships and drug design. Pharmacokinet Theory Methodol Int Encycl Pharmacol Ther Sect 122:311–368

33. Xu C, Li CY-T, Kong A-NT (2005) Induction of phase I, II and III drug metabolism/transport by xenobiotics. Arch Pharm Res 28:249. https://doi.org/10.1007/BF02977789

34. Schlichting I, Berendzen J, Chu K, Stock AM, Maves SA, Benson DE, Sweet RM, et al (2000) The catalytic pathway of cytochrome p450cam at atomic resolution. Science 287:1615–1622

35. Banoglu E (2000) Current status of the cytosolic sulfotransferases in the metabolic activation of promutagens and procarcinogens. Curr Drug Metab 1:1–30

36. Anzenbacher P, Anzenbacherová E (2001) Cytochromes P450 and metabolism of xenobiotics. Cell Mol Life Sci C 58:737–747. https://doi.org/10.1007/PL00000897

37. Food US (1997) Drug Administration Guidance for Industry, Drug Metabolism/Drug Interaction Studies in the Drug Development Process: Studies in vitro. Cent. Drug Eval. Res.

38. Bjornsson TD, Callaghan JT, Einolf HJ, Fischer V, Gan L, Grimm S, Kao J, et al (2003) The conduct of in vitro and in vivo drug-drug interaction studies: a Pharmaceutical Research and Manufacturers of America (PhRMA) perspective. Drug Metab Dispos 31:815–832

39. Roncaglioni A, Toropov AA, Toropova AP, Benfenati E (2013) In silico methods to predict drug toxicity. Curr Opin Pharmacol 13:802–806. https://doi.org/https://doi.org/10.1016/j.coph.2013.06.001

40. (2013) Scientific Working Group for Forensic Toxicology (SWGTOX) Standard Practices for Method Validation in Forensic Toxicology. J Anal Toxicol 37:452–474.

https://doi.org/10.1093/jat/bkt054

41. Swortwood MJ, Carlier J, Ellefsen KN, Wohlfarth A, Diao X, Concheiro-Guisan M, Kronstrand R, et al (2016) In vitro, in vivo and in silico metabolic profiling of α-pyrrolidinopentiothiophenone, a novel thiophene stimulant. Bioanalysis 8:65–82. https://doi.org/10.4155/bio.15.237

42. Diao X, Carlier J, Zhu M, Pang S, Kronstrand R, Scheidweiler KB, Huestis MA (2017) In vitro and in vivo human metabolism of a new synthetic cannabinoid NM-2201 (CBL-2201). Forensic Toxicol 35:20–32. https://doi.org/10.1007/s11419-016-0326-9

43. Kevin RC, Lefever TW, Snyder RW, Patel PR, Fennell TR, Wiley JL, McGregor IS, et al (2017) In vitro and in vivo pharmacokinetics and metabolism of synthetic cannabinoids CUMYL-PICA and 5F-CUMYL-PICA. Forensic Toxicol 35:333–347. https://doi.org/10.1007/s11419-017-0361-1

44. Gandhi AS, Wohlfarth A, Zhu M, Pang S, Castaneto M, Scheidweiler KB, Huestis MA (2015) High-resolution mass spectrometric metabolite profiling of a novel synthetic designer drug, N-(adamantan-1-yl)-1-(5-fluoropentyl)-1H-indole-3-carboxamide (STS-135), using cryopreserved human hepatocytes and assessment of metabolic stability with human liv. Drug Test Anal 7:187–198

45. Hess C, Schoeder CT, Pillaiyar T, Madea B, Müller CE (2016) Pharmacological evaluation of synthetic cannabinoids identified as constituents of spice. Forensic Toxicol 34:329–343. https://doi.org/10.1007/s11419-016-0320-2

46. Banister SD, Longworth M, Kevin R, Sachdev S, Santiago M, Stuart J, Mack JBC, et al (2016) Pharmacology of Valinate and tert-Leucinate Synthetic Cannabinoids 5F-AMBICA, 5F-AMB, 5F-ADB, AMB-FUBINACA, MDMB-FUBINACA, MDMB-CHMICA, and Their Analogues. ACS Chem Neurosci 7:1241–1254. https://doi.org/10.1021/acschemneuro.6b00137

47. Andersson M, Diao X, Wohlfarth A, Scheidweiler KB, Huestis MA (2016) Metabolic profiling of new synthetic cannabinoids AMB and 5F-AMB by human hepatocyte and liver microsome incubations and high-resolution mass spectrometry. Rapid Commun

Mass Spectrom 30:1067–1078. https://doi.org/10.1002/rcm.7538

48. Wohlfarth A, Castaneto MS, Zhu M, Pang S, Scheidweiler KB, Kronstrand R, Huestis MA (2015) Pentylindole/Pentylindazole Synthetic Cannabinoids and Their 5-Fluoro Analogs Produce Different Primary Metabolites: Metabolite Profiling for AB-PINACA and 5F-AB-PINACA. AAPS J 17:660–677. https://doi.org/10.1208/s12248-015-9721-0

49. Wiley JL, Marusich JA, Lefever TW, Antonazzo KR, Wallgren MT, Cortes RA, Patel PR, et al (2015) AB-CHMINACA, AB-PINACA, and FUBIMINA: Affinity and Potency of Novel Synthetic Cannabinoids in Producing Δ9-Tetrahydrocannabinol{\textendash}Like Effects in Mice. J Pharmacol Exp Ther 354:328–339. https://doi.org/10.1124/jpet.115.225326

50. Mogler L, Franz F, Rentsch D, Angerer V, Weinfurtner G, Longworth M, Banister SD, et al (2018) Detection of the recently emerged synthetic cannabinoid 5F–MDMB-PICA in ‘legal high’ products and human urine samples. Drug Test Anal. https://doi.org/10.1002/dta.2201

51. Carlier J, Diao X, Scheidweiler KB, Huestis MA (2017) Distinguishing Intake of New Synthetic Cannabinoids ADB-PINACA and 5F-ADB-PINACA with Human Hepatocyte Metabolites and High-Resolution Mass Spectrometry. Clin Chem. https://doi.org/10.1373/clinchem.2016.267575

52. Yeter O, Erol Öztürk Y Metabolic profiling of synthetic cannabinoid 5F-ADB by human liver microsome incubations and urine samples using high-resolution mass spectrometry. Drug Test Anal 0:. https://doi.org/10.1002/dta.2566

Appendix 1

Supplementary Table 1: Agilent 6470A LC method properties

Time (mins)	A %	B %	Flow(mL/min)
0.0	90.0	10	0.3
0.6	90.0	10.0	0.3
1.5	85.0	15.0	0.3
2.0	80.0	20.0	0.3
2.5	70.0	30.0	0.3
3.0	65.0	35.0	0.3
3.5	60.0	40.0	0.3
4.0	55.0	45.0	0.3
4.5	52.5	47.5	0.3
5.0	50.0	50.0	0.3
5.5	45.0	55.0	0.3
5.75	42.5	57.5	0.3
5.85	41.5	58.5	0.3
6.0	40.0	60.0	0.3
6.5	35.0	65.0	0.3
8.5	20.0	80.0	0.3
10.5	5.0	95.0	0.3
13.5	90.0	10.0	0.3

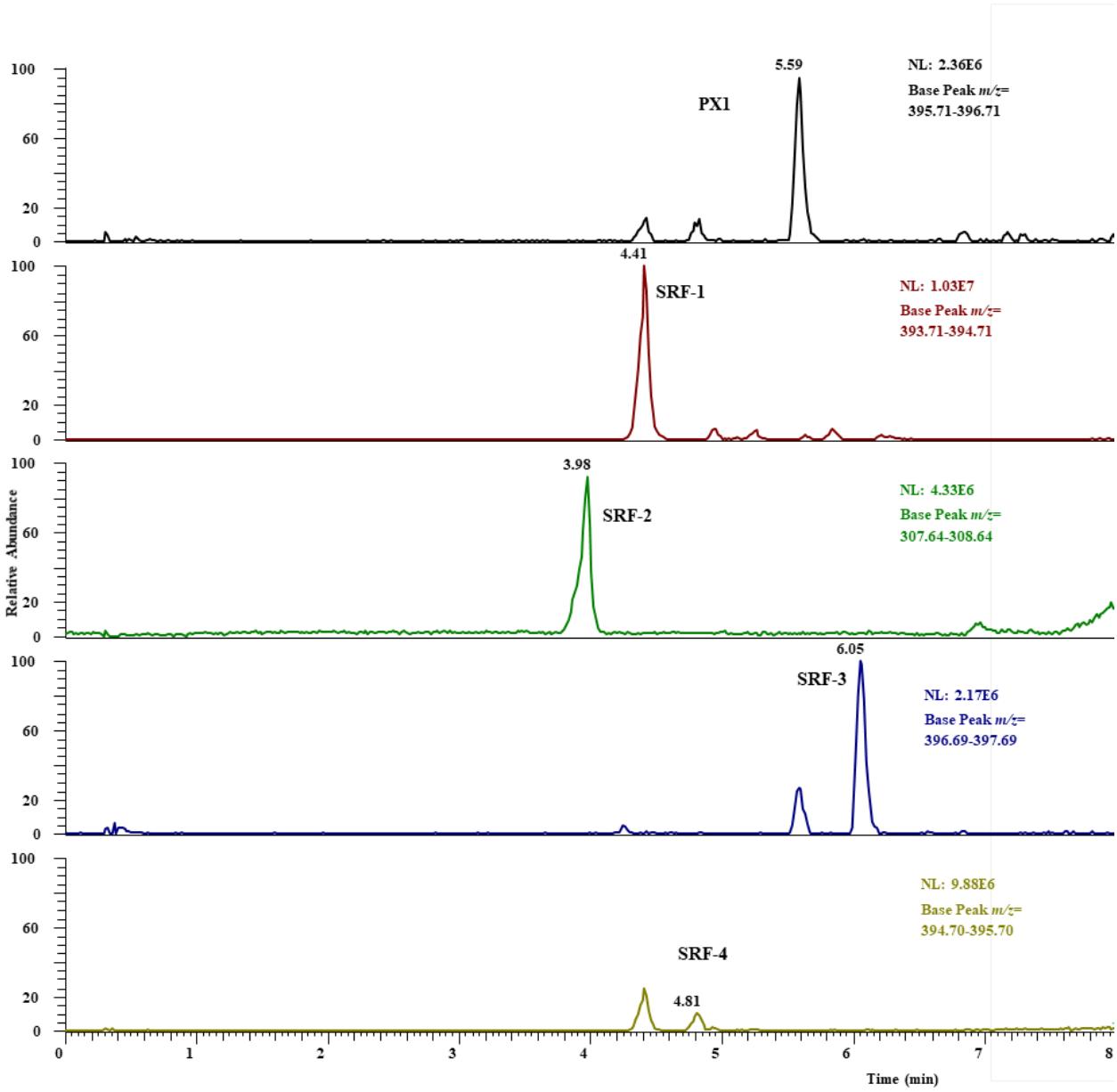

Figure 7: PX-1and metabolites chromatogram.

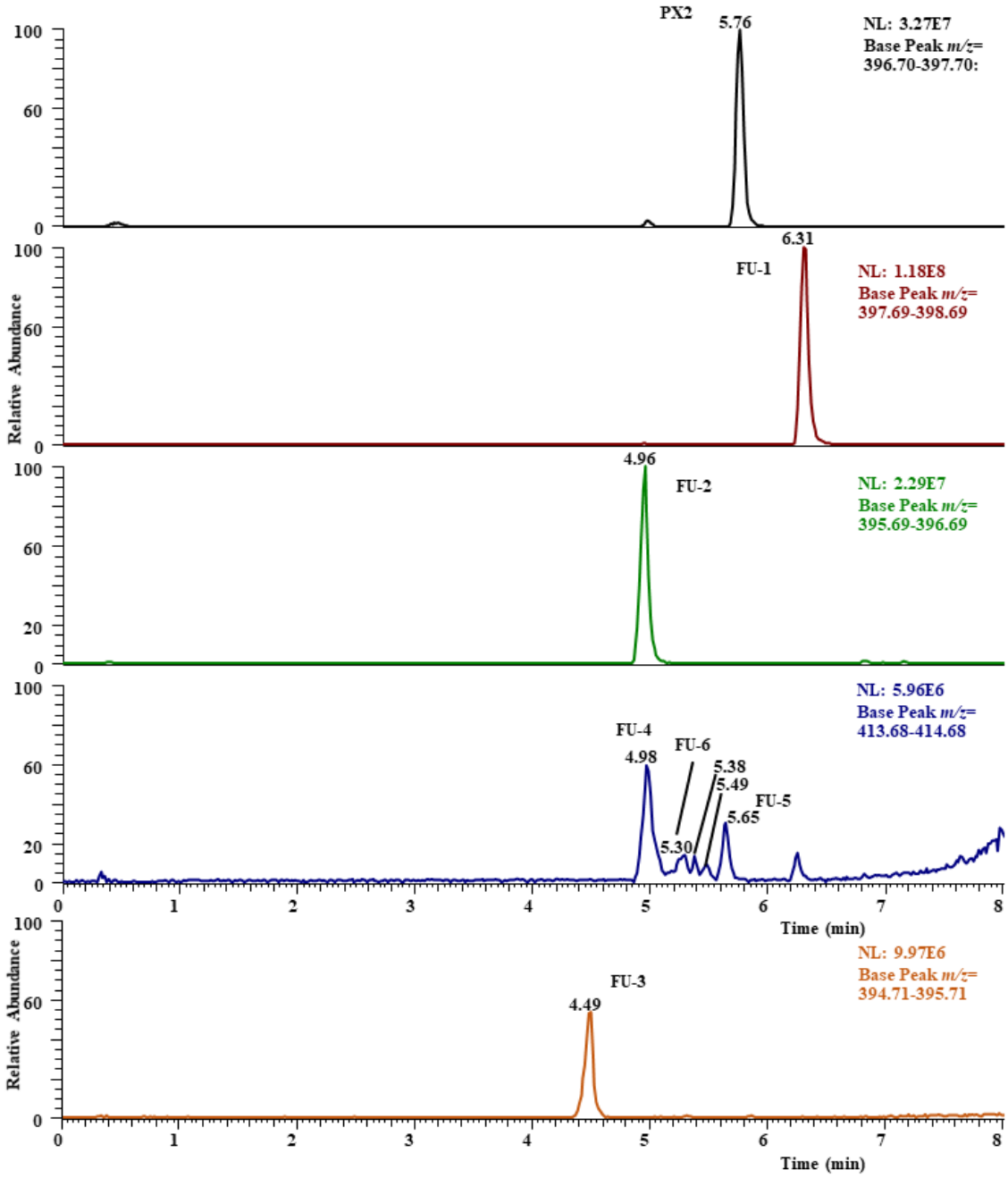

Figure 8: PX-2 and metabolites chromatogram.

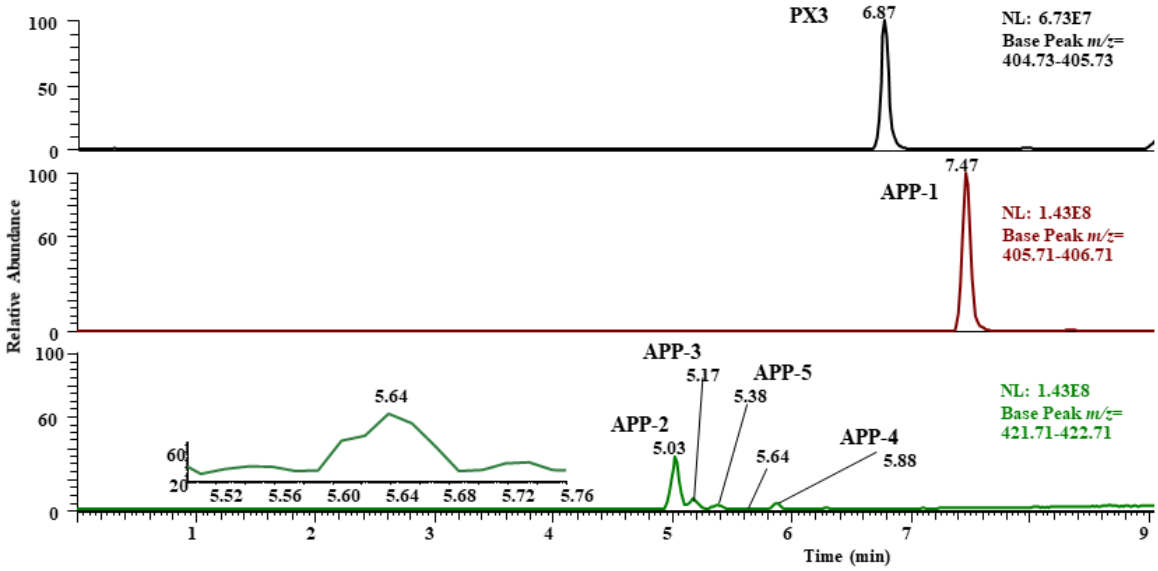

Figure 9: PX-3 and metabolites chromatogram.

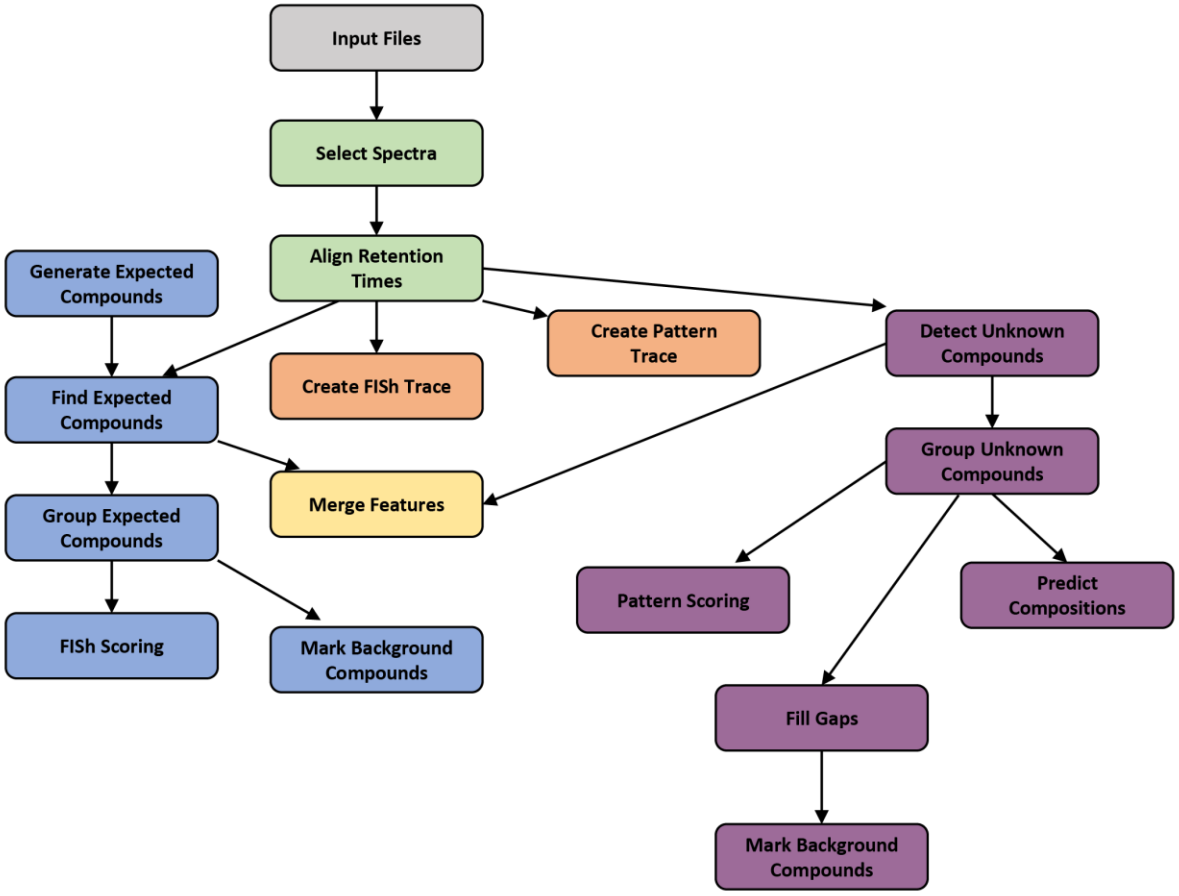

Figure 10: Compound Discoverer Workflow.

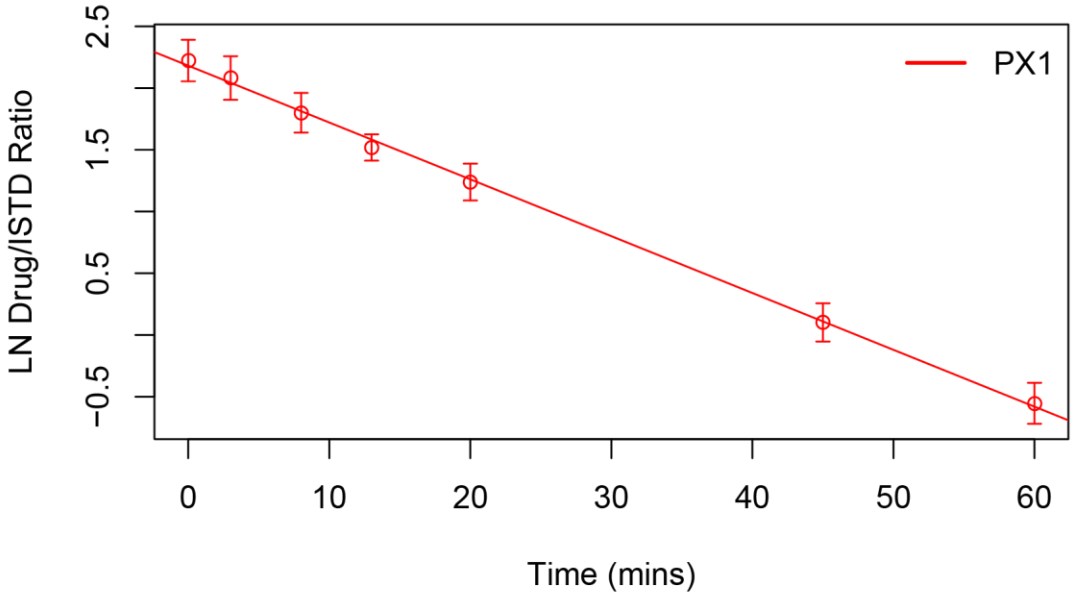

Figure 11: Half-life of PX-1.

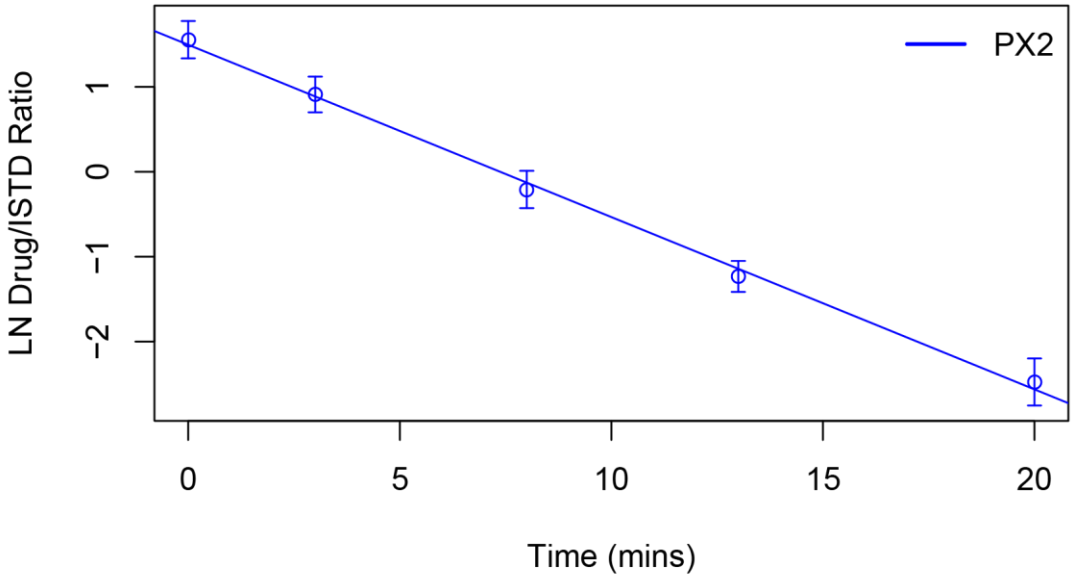

Figure 12: Half-life of PX-2.

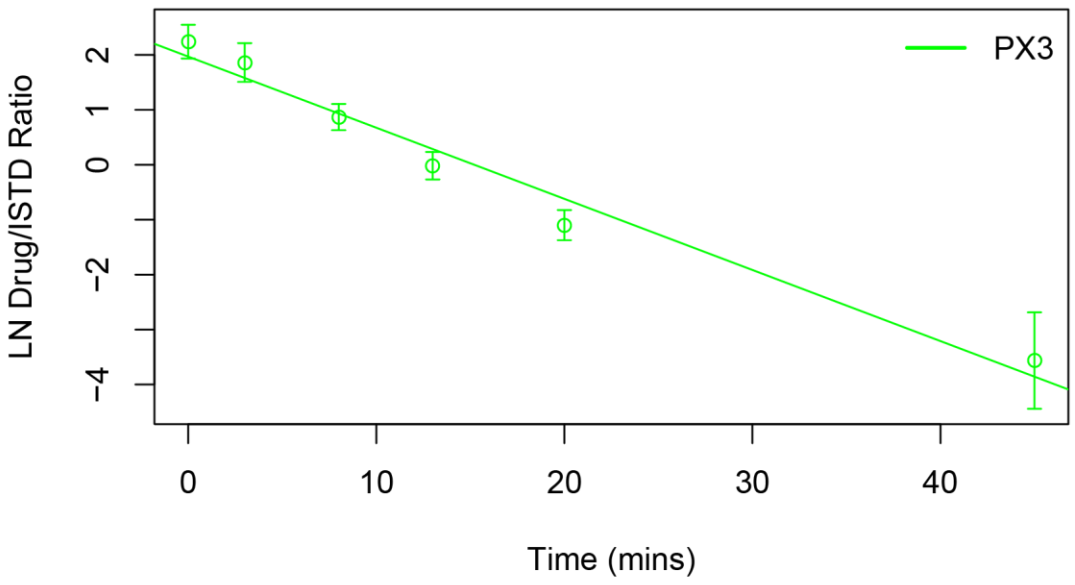

Figure 13: Half-life of PX-3.